## Chapter 4

# Compensatory lipid metabolism in the skin of apolipoprotein AI deficient mice in response to hypoalphalipoproteinemia

*Manuscript in preparation*

Renata Martins Cardoso[1], Samira Absalah[1], Menno Hoekstra[1], Joke A. Bouwstra[1*], Miranda Van Eck[1*]

[1]Division of BioTherapeutics, Leiden Academic Centre for Drug Research, Leiden University, Leiden, The Netherlands

*Both authors contributed equally

**ABSTRACT**

High-density lipoproteins (HDL) have a vital function in cholesterol metabolism. It involves a heterogeneous group of relatively small cholesterol-transporting particles that can efficiently traffic from plasma to interstitial fluid of various tissues, including the skin, and vice versa. . The importance of HDL for the transport of lipids into skin or efflux of excess lipids, produced by keratinocytes, out of the skin is currently unknown. In this study, we aimed to assess the impact of strongly reduced HDL levels (hypoalphalipoproteinemia) on skin lipid homeostasis. For that purpose, the skin of apolipoprotein AI knockout (*APOAI*$^{-/-}$) mice was compared to control wild type mice of the same age with particular focus on epidermal barrier lipids and the mRNA expression of enzymes involved in their synthesis. Despite the substantial decrease in plasma levels of cholesterol and triglycerides, *APOAI* deficiency did not affect the general morphology of the skin. Detailed analysis of the epidermal barrier lipids showed comparable cholesterol levels and ceramide and free fatty acid compositions between control and *APOAI*$^{-/-}$ mice. However, the unaltered barrier lipid composition did coincide with an increased expression of genes involved in cholesterol synthesis (*HMGCR, HMGCS1*), cholesterol uptake from lipoproteins (*LDLR, SR-BI*) and free fatty acid synthesis (*FAS, ACC*) in the skin of *APOAI*$^{-/-}$ mice. In summary, this study shows that neither the morphology or the epidermal lipid composition and organization of the skin of *APOAI*$^{-/-}$ mice is affected by hypoalphalipoproteinemia. A local compensatory mechanism marked by upregulation of lipid synthesis genes preserving the epidermal lipid profile in absence of HDL, suggests that HDL likely plays an important role in the delivery of essential lipids to the skin.

***Keywords:*** *skin barrier lipids; apolipoprotein AI knockout; high-density lipoprotein; skin lipid metabolism*

## 1. INTRODUCTION

Apolipoprotein AI (APOAI) is the main protein component of high-density lipoprotein (HDL), a heterogeneous group of particles involved in the transport of cholesterol throughout the body[1,2]. APOAI is produced by enterocytes and hepatocytes and secreted into the plasma in a lipid-poor form[1,2]. Following interaction with ATP-binding cassette (ABC) transporter A1, plasma lipid-poor APOAI quickly acquires phospholipids and free cholesterol to form nascent HDL particles[2]. Maturation of nascent HDL continues with uptake of more lipids from peripheral tissues via ABCA1, ABCG1, and scavenger receptor class B member I (SR-BI) as well as by exchange from other lipoproteins[3]. The enzyme lecithin: cholesterol acyl transferase (LCAT) is a key player in the maturation of HDL particles as it generates cholesteryl esters (CE) for storage in the lipoprotein core[3,4].



HDL particles are relatively small and can efficiently traffic from plasma to interstitial fluid of various tissues, including the skin, and vice versa. In fact, both human and murine keratinocytes express ABCA1, ABCG1, cluster of differentiation 36 (CD36), and SR-BI facilitating the transit of lipids to and from HDL particles[5–7]. Lipids are key components of the stratum corneum (SC), the outermost dead layer of the skin, an organ that functions as a protective barrier in the interface between the body and the environment. The SC is mainly composed of cholesterol, free fatty acids (FFAs) and ceramides (CERs). Although most of the SC lipids are synthesized by keratinocytes[8], lipids of extracutaneous origin can be found in the skin[7,9–11], which are likely acquired via lipoprotein receptors expressed in keratinocytes (*e.g.* low-density lipoprotein receptor, SR-BI, and CD36)[7,10,12].

Recently, we have demonstrated that the skin of young adult *SR-BI* knockout (*SR-BI* $^{-/-}$) mice displayed an altered epidermal lipid composition and reduced lipid barrier functionality[13]. In these mice, SR-BI is not only absent in keratinocytes, but also in liver, the primary site for removal of HDL-CE from the circulation. As a result, the metabolism of HDL is severely impaired in SR-BI deficient mice, leading to augmented HDL cholesterol levels in the circulation (hyperalphalipoproteinemia).

In contrast, deficiency of APOAI leads to a virtual absence of HDL in the circulation, thereby impairing the transport of lipids (cholesterol, triglycerides) from peripheral tissues to the plasma via HDL particles[2]. Over 40 *APOAI* gene defects have been described in humans, which among others impact interactions with ABCA1 and/or activation of LCAT and severely affect HDL metabolism, leading to an increased risk for cardiovascular diseases[14–19]. Remarkably, enzymatic colorimetric analysis of whole

skin of *APOAI*$^{-/-}$ mice did not reveal changes in the overall cholesterol, phospholipids, and triglycerides contents[20]. However, the impact of the severely reduced HDL levels on specifically epidermal barrier lipids (CERs, FFAs) has not yet been assessed. Additionally, considering the large amount of HDL transiting through the skin via the vascular bed[21] and the epidermal barrier lipid alterations reported in *SR-BI*$^{-/-}$ mice[13], it is important to obtain more detailed insight in whether lipid metabolism is changed in the skin of *APOAI*$^{-/-}$ mice, in which HDL particles are virtually absent.

In the present study, the skin of *APOAI*$^{-/-}$ mice was compared to that of wild type (WT) mice to gain insight into skin lipid metabolism under conditions of an HDL-deficient hypolipidemic profile (hypoalphalipoproteinemia). Hereto, the epidermal lipid composition and organization were determined and the expression of genes involved in the local lipid synthesis and uptake was measured. The skin of *APOAI*$^{-/-}$ mice showed comparable epidermal barrier lipid composition and organization to the WT mice. However, gene expression analysis revealed that in *APOAI*$^{-/-}$ mice various genes related to lipid synthesis in the skin were upregulated, indicating a compensatory increase in local lipid synthesis.

## 2. MATERIALS AND METHODS

### 2.1 Chemicals

Rodent chow diet, low in fat and cholesterol (Rat and Mouse No.3 breeding diet), was purchased from Special Diets Services (United Kingdom). Ketamine and atropine from AUV Veterinary Services (Cuijk, The Netherlands). Xylazine from ASTFarma (Oudewater, The Netherlands). Sodium chloride (NaCl) from Boom (Meppel, The Netherlands). Sodium phosphate dibasic ($Na_2HPO_4$), hematoxylin, eosin, trypsin from bovine pancreas, trypsin inhibitor, cholesterol, FFA C16-C30, deuterated FFA C18 and deuterated FFA C24, chloroform, deuterated water ($D_2O$), natrium bromibe (NaBr), were purchased from Sigma-Aldrich (Zwijndrecht, The Netherlands). Potassium dihydrogen phosphate ($KH_2PO_4$), potassium chloride (KCl) and Entellan® were purchased from Merck (Darmstadt, Germany). CER[NS] (C24deuterated; C18protonated) and all synthetic CERs were kindly provided by Evonik Industries (Essen, Germany). Heptane was purchased from ChemLab (Zedelgem, Belgium). Methanol, ethanol and isopropanol were purchased from Biosolve (Valkenswaard, The Netherlands). All solvents used were analytical grade.

### 2.2 Animals

16-18 weeks old female C57BL/6 WT mice were obtained from The Jackson laboratory and bred at the Gorlaeus laboratories (Leiden, The Netherlands). Homozygous apolipoprotein AI knockout (*APOAI*$^{-/-}$) mice were rederived from *APOAI*/*LDLR* double knockout mice (C57Bl/6J background; kindly provided by Dr. Jan Albert Kuivenhoven, Department of Experimental Vascular Medicine, Academic Medical Centre, Amsterdam) by crossbreeding with C57BL/6 mice and subsequent intercrossing of the offspring[22]. All mice were kept under standard laboratory conditions at 20°C and with light cycle of 12h light/12h dark. The mice had access to water and standard low fat chow diet ad libitum. The non-fasted mice were anesthetized with a mixture of xylazine (70 mg/kg body weight); atropine (1.8 mg/kg body weight) and ketamine (350 mg/kg body weight) for retro-orbital bleeding. Next, the mice were perfused with phosphate buffered saline (PBS at pH 7.4; 8.13 g/L NaCl, 2.87 g/L $Na_2HPO_4$, 0.2 g/L $KH_2PO_4$, 0.19 g/L KCl in milliQ water) and the skin of their back was collected. All experiments were performed in agreement with National guidelines and approved by the Ethics Committee for Animals Experiments of Leiden University.

### 2.3 Plasma lipid analysis

Enzymatic colorimetric assays (Roche Diagnostics, Almere, Netherlands) were used to measure non-fasted plasma levels of free cholesterol (FC), cholesteryl esters (CE) and triglycerides as described previously[23].

### 2.4 Skin morphology staining

Paraffin embedded skin sections (4-5 μm) were deparaffinized, rehydrated and stained with hematoxylin and eosin according to manufacturer's instructions. Stained slides were mounted in Entellan® and imaged with a Zeiss Axioplan 2 light microscope (Zeiss, Best, The Netherlands).

### 2.5 Epidermis isolation

Skin samples without hypodermis were placed on a paper filter soaked with 0.3% w/v trypsin solution in PBS with the dermis side in contact with the paper. The skin was kept overnight at 4°C and, on the next day; the samples were incubated at 37°C for trypsin activity. After 1 hour the epidermis was separated and subsequently rinsed with trypsin inhibitor (0.1% w/v inhibitor in PBS) and in demi-water. The samples were dried overnight at room temperature and stored under argon atmosphere in a

container containing silica and protected from light until epidermal lipid extraction and FTIR measurements.

### 2.6 Lipid extraction and liquid chromatography-mass spectrometry (LC/MS)

Epidermal lipids were extracted as described by Boiten *et. al.* (2016)[24] and stored in chloroform:methanol (2:1; v/v) at 4°C under argon atmosphere for analysis of cholesterol, CERs, and FFAs using an Acquity UPLC H-class system (Waters, Milford, MA, USA) connected to an XEVO TQ-S mass spectrometer (MS; Waters, Milford, MA, USA) with an atmospheric pressure chemical ionization (APCI) chamber, as previously described[13,25]. In short, for cholesterol and CERs analysis, deuterated CER NS (C24 acyl chain deuterated; C18 sphingoid base protonated) was added as internal standard to all samples prior to injection into the UPLC/MS system. Upon completion of the measurements, the area under the curve (AUC) was determined using Software Waters MassLynx 4.1 for both cholesterol and CER analyses. Cholesterol AUC was divided by internal standard and further corrected for the response based on a calibration curve of cholesterol and the data was plotted as absolute amount of cholesterol (µg) per epidermis weight (mg). CER AUC data was divided by internal standard and plotted as relative percentage of ceramide subclasses calculated. In this work, CERs are named as according to Motta *et. al.* (1993) describing the acyl chain (non-hydroxy fatty acid [N]; α-hydroxy fatty acid [A]; esterified ω-hydroxy fatty acid [EO]) and the sphingoid base (dihydrosphingosine, [dS]; sphingosine [S]; phytosphingosine [P])[26]. For FFAs analysis, deuterated FFA C18 and FFA C24 were used as internal standard to all samples. The AUC was corrected by the internal standard FFA C24 and for the response based on calibration curves of FFA C16-C30. The data was plotted as absolute amounts and relative mass percentage to the total FFA content detected. Due to manufacturer's contamination of the chloroform extracting solvent with FFA C16:0 and C18:0, these FFAs were not determined. Their respective unsaturated species were not plotted as they are important components of sebum lipids.

### 2.7 Fourier transformed infrared spectroscopy (FTIR)

Fourier transformed infrared spectroscopy (FTIR) measurements were performed using a Varian 670-IR spectrometer (Agilent Technologies, Inc., Santa Clara, CA) equipped with a broad-band mercury cadmium telluride detector. Prior the measurement, the epidermis was hydrated for 24 hours in a deuterated water solution containing 27% w/v sodium bromide. Next, the epidermis was mounted between 2 silver bromide windows and FTIR spectra (600-4000 $cm^{-1}$) were collected with resolution of 1 $cm^{-1}$ in a temperature range from 0-90°C (0.5°C/min). The spectra were deconvoluted (half

width of 4 $cm^{-1}$; enhancement factor of 1.7) and further processed with Resolutions Pro 4.1 (Varian Inc.) software. Lateral organization of the epidermal lipids was examined by analysis of the $CH_2$ rocking vibrations (710-740 $cm^{-1}$). The end of the orthorhombic to hexagonal phase transition was determined by the disappearance of the peak at 730 $cm^{-1}$.

### 2.8 qPCR

Total RNA was isolated from skin samples without hypodermis[27]. RNA (1 µg) was transcribed to cDNA using with M-MuLV reverse transcriptase. Quantitative gene analysis was done with QuantStudio 6 Flex Real-time PCR systems (Applied Biosystems, Foster City, CA, USA) using SYBR Green Technology for detection. Ribosomal protein, large, P0 (*RPL0*) and ribosomal protein L37 (*RPL37*) were used as reference genes. Relative gene expression was determined by subtracting the average threshold cycle (Ct) of the reference genes from the Ct of the target gene and raising the difference to 2 to the power. Gene expression was plotted as relative fold change compared to the WT control group. Primer sequences used in the gene expression analysis are available in Supplementary Table S1.



### 2.9 Statistical analysis

Data are presented as mean±standard deviation (SD). Statistical analysis was performed using GraphPad Prism 8 (GraphPad Software Inc., CA, USA). *P* values below 0.05 were considered significant.

## 3. RESULTS

### 3.1 *APOAI* deficiency in mice lowers plasma cholesterol without altering skin morphology

The non-fasted plasma lipid profile of WT and *APOAI*$^{-/-}$ mice was determined by enzymatic colorimetric assays to measure triglycerides, free cholesterol (FC), and cholesteryl esters (CE) (Fig 1a). *APOAI*$^{-/-}$ mice on low-fat chow diet showed reduced triglycerides levels (0.8±0.2 µg/ml plasma) compared to the WT control (1.1±0.1 µg/ml plasma) ($p<0.05$). The absence of *APOAI* leads to a strong reduction in circulating HDL-cholesterol[20]. As a result, *APOAI*$^{-/-}$ mice showed a large reduction in the FC fraction (0.23±0.05 µg/ml plasma) and CE fraction (0.31±0.05 µg/ml plasma) compared to the WT counterparts (0.36±0.05 µg/ml ($p<0.01$) and 0.86±0.08 µg/ml plasma ($p<0.0001$), respectively). Next, the morphology of the skin of WT and *APOAI*$^{-/-}$ mice was assessed by

hematoxylin and eosin staining (Fig 1b). Overall, the morphology of the *APOAI*$^{-/-}$ skin was comparable to the WT control with similar SC and epidermal and dermal morphology. At general inspection no signs of inflammation were observed (*e.g.* epidermal thickening).

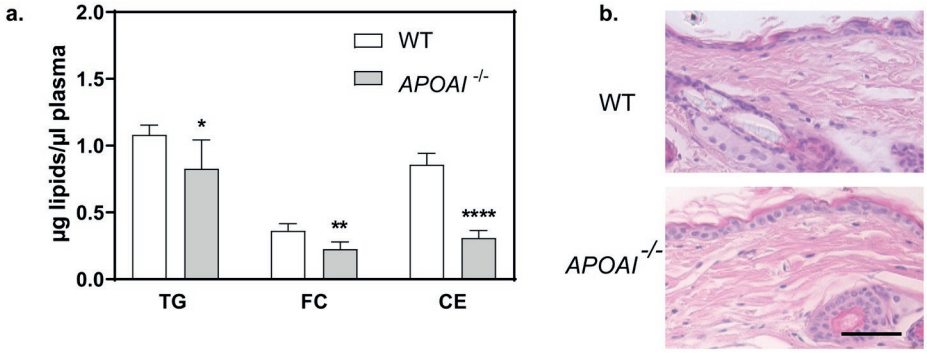


**Figure 1. Deficiency of *APOAI* in young adult mice reduces plasma lipid levels but does not affect skin morphology.** Non-fasted (a) plasma levels of triglycerides (TG); free cholesterol (FC) and cholesteryl esters (CE) were measured by enzymatic colorimetric reactions (n=5-6 animals/group) and (b) hematoxylin and eosin staining of paraffin skin sections of wild type (WT) and *APOAI* knockout (*APOAI*$^{-/-}$) mice. Representative micrographs (Scale bar = 50 µm). Data shown as mean ± SD. Significant differences between groups were determined by two-tailed unpaired Student's T-test; *$p$<0.05, **$p$<0.01 and ****$p$<0.0001.

### 3.2 Absence of *APOAI* minimally affects the epidermal lipid composition

The three main types of epidermal barrier lipids (cholesterol, CERs, and FFAs) were analyzed by LC/MS. The cholesterol content in the epidermis of *APOAI*$^{-/-}$ mice (30.7±1.3 µg/mg epidermis) was comparable to the WT control (28.7±3.1 µg/mg epidermis) (Fig 2a). Seven CER subclasses were detected in the epidermis of both types of mice (Fig 2b): CER NdS, CER NS, CER NP/AdS, CER AS, CER EOS, CER EOdS, nomenclature according to Motta *et. al.* (1993)[26]. The subclasses CER NP and CER AdS could not be completely separated in our method; thus, these CER subclasses are depicted in one group. In *APOAI*$^{-/-}$ mice, the percentage CER NdS was increased (42.3±1.5% versus 39.7±0.5% in WT, $p$<0.01), while the percentage of CER AS (11.1±0.9%) was lower in the *APOAI*$^{-/-}$ mice as compared to WT controls (13.5±1.1%; $p$<0.05). The abundance of CER NS, CER NP/AdS, CER EOdS and CER EOS was similar between groups. The total absolute FFA content did not differ between groups (Supplementary Fig S1a); hence the relative FFA composition in the epidermis of *APOAI*$^{-/-}$ mice was equivalent to that of WT controls (Fig 2c). In both groups of mice, FFA C24:0 and FFA C26:0 were the most abundant species, comprising nearly 70% of the total FFA content. Although no significant differences

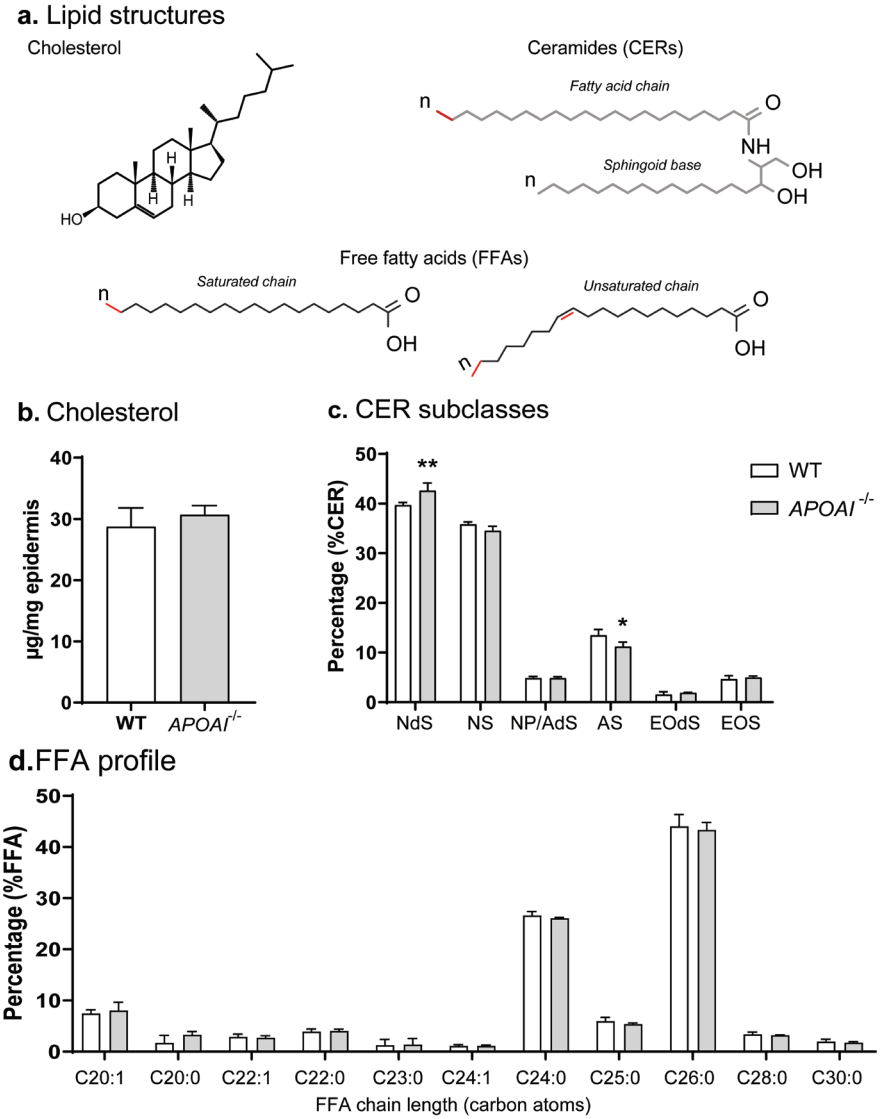


**Figure 2. The epidermal lipid composition is minimally altered in young adult mice lacking *APOAI*.** Epidermal lipids in wild type (WT) and *APOAI* knockout (*APOAI*$^{-/-}$) mice were analyzed by LC/MS: (a) the structure of the three main barrier lipids present in the skin, (b) cholesterol content, (c) CERs (CER subclasses: NdS, NS, NP/AdS, AS, EOdS, EOS) and (d) FFAs with chain length from 20-30 carbon atoms. CER subclasses named according to Motta *et. al.* (1993) describing the acyl chain (non-hydroxy fatty acid [N]; α-hydroxy fatty acid [A]; esterified ω-hydroxy fatty acid [EO]) and the sphingoid base (dihydrosphingosine, [dS]; sphingosine [S]; phytosphingosine [P]) 26. CER NP and CER AdS are represented together as these subclasses could not be fully separated. Data shown as mean±SD; n=3/group. Statistical significance was calculated by two-tailed unpaired Student's T-test and Two-way ANOVA followed by Holm-Šídák post-hoc test; *$p$<0.05; **$p$<0.01.

were noted between the FFA profiles, the epidermis of *APOAI*$^{-/-}$ mice showed a slight shift towards shorter FFA chains (below 24 carbon atoms), which comprised 19.3±1.3% of the total FFA species versus 17.1±0.8% in WT ($p$=0.058) (Supplementary Fig S1b). The ratio between unsaturated and saturated FFAs was comparable in both groups (0.13±0.02 in WT and 0.13±0.03 in *APOAI*$^{-/-}$ mice, (Supplementary Fig S1c).

### 3.3 Epidermal lipids in the skin of *APOAI*$^{-/-}$ mice adopt an orthorhombic organization

For the functionality of the skin barrier not only the lipid composition is of importance, but also the lateral organization of these lipids. Therefore next the lateral lipid organization in the skin of WT and *APOAI*$^{-/-}$ mice was analyzed by FTIR at temperatures ranging from 0°C to 50°C. At low temperatures, the $CH_2$ rocking vibrations (710-740 $cm^{-1}$) showed a doublet at 710 $cm^{-1}$ and at 730 $cm^{-1}$ for WT and *APOAI*$^{-/-}$ epidermis (Fig 3). The presence of the doublet in this region of the spectrum represents orthorhombic lateral packing, which was also present at normal skin surface temperature (~32°C) (Fig 3; red line)[28–30]. The temperature at which the lateral lipid organization shifts from orthorhombic to hexagonal was determined by the disappearance of the peak at 730 $cm^{-1}$ as a function of temperature. The lipids in the epidermis of WT and *APOAI*$^{-/-}$ mice showed a shift towards the hexagonal phase at temperatures varying from 38°C to 42°C.

### 3.4 Skin of *APOAI*$^{-/-}$ mice shows adaptive expression of lipid synthesis genes in response to hypoalphalipoproteinemia

Altered plasma lipid profiles have been reported to affect the epidermal lipid composition[31–33]. To understand how the epidermal lipid composition was largely maintained in *APOAI*$^{-/-}$ mice despite the severe hypoalphalipoproteinemia, next the expression of genes involved in lipid synthesis and lipid uptake were determined. Regarding the synthesis of cholesterol, the expression of *HMGCR* (encoding for the enzyme 3-hydroxy-3-methyl-glutaryl-coenzyme A reductase) and *HMGCS1* (encoding for the enzyme 3-Hydroxy-3-Methylglutaryl-CoA Synthase 1) were strongly upregulated in *APOAI*$^{-/-}$ mice (1.9-fold and 1.7-fold increase, respectively) as compared to WT mice ($p$<0.01) (Fig 4a). Also, mRNA levels of plasma lipoprotein receptors *LDLR* (1.4-fold) and *SR-BI* (2.5-fold) were significantly higher in *APOAI*$^{-/-}$ mice (Fig 4a).

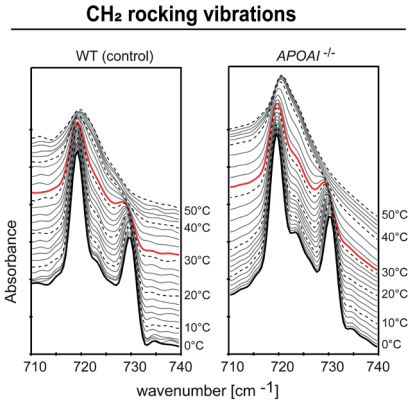


**Figure 3. Epidermal lipids in *APOAI*$^{-/-}$ mice show orthorhombic lateral organization.** Lateral packing of the epidermal lipids of wild type (WT) and *APOAI* knockout (*APOAI*$^{-/-}$) mice was assessed by FTIR using the spectrum in the CH2 rocking vibrations (710-740 cm$^{-1}$) plotted as a function of temperature (0-50°C). Lateral organization at skin temperature (~32°C) is indicated by the red line. Spectra are representative of 3-4 animals/group.



Analysis of FFA chain elongases in *APOAI*$^{-/-}$ skin revealed lower levels of *ELOVL1* (55% reduction, $p<0.01$), while the expressions of *ELOVL4* and *ELOVL6* remained unaltered (Fig 4c and Supplementary Fig S2). *SCD1* expression (encoding for stearoyl-CoA desaturase 1 involved in FFA desaturation) was similar in both groups of mice (Fig 4c). Interestingly, skin levels of *DGAT2*, a gene encoding for the enzyme diacylglycerol O-acyltransferase 2 involved in the synthesis of triglycerides, showed nearly 45% reduction ($p<0.01$) in the hypolipidemic *APOAI*$^{-/-}$ mice. In agreement with the upregulation of lipid synthesis genes, the levels of *IVL* (encoding for involucrin, a marker for keratinocyte differentiation) were increased by 40% ($p<0.05$) in the *APOAI*$^{-/-}$ mice; yet, *K10* expression (encoding for keratin 10, an early marker for keratinocyte differentiation) was comparable to the WT controls (Supplementary Fig S2).

## 4. DISCUSSION

In the present work, we analyzed the detailed composition and organization of the barrier lipids in hypolipidemic *APOAI*$^{-/-}$ mice and associated our findings with the expression of genes involved in lipid synthesis in the skin. Our data showed that the lipid composition and packing in the SC lipid matrix were preserved in *APOAI* deficient mice. More importantly, we demonstrated at gene expression level that compensatory mechanisms regulating local lipid synthesis and uptake likely contribute to the maintenance of skin lipid homeostasis.

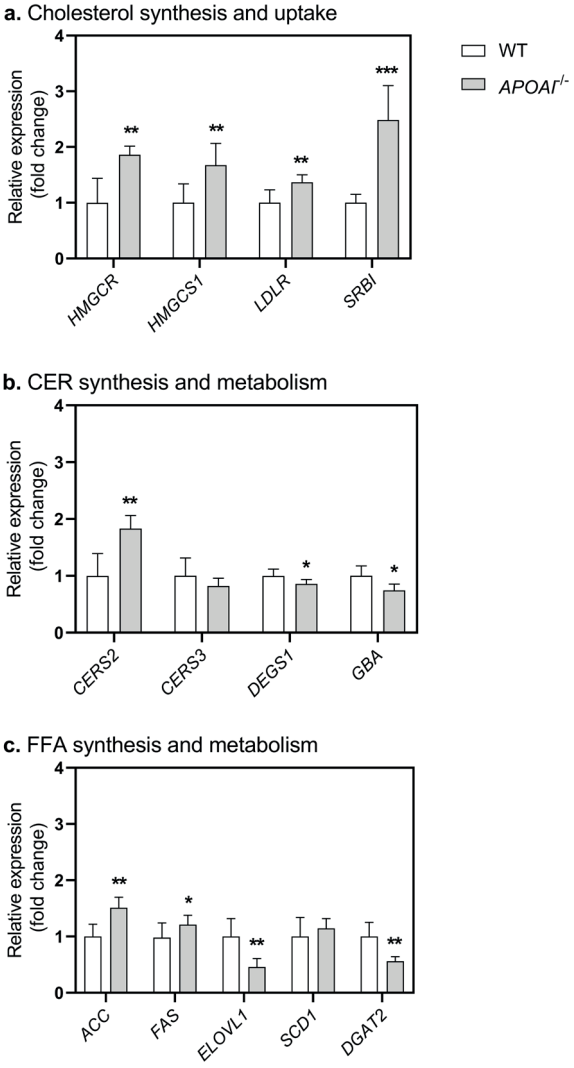


**Figure 4. *APOAI* deficiency alters expression profile of various genes involved in lipid synthesis and uptake in the skin.** Relative mRNA expression of genes related to (a) cholesterol; (b) CER and (c) FFA synthesis were determined in the epidermis of wild type (WT) and *APOAI* knockout (*APOAI*$^{-/-}$) mice. Data shown as mean±SD and plotted as fold change expression compared to the WT control (n=5-6 animals/group). Statistical significance was determined by two-tailed unpaired Student's t-Test. *$p$<0.05; **$p$<0.01; ***$p$<0.001.

HDL accounts for the largest fraction of lipoproteins in the plasma of WT mice, with APOAI being the major apolipoprotein in these particles[2,34]. In mice lacking APOAI, HDL

is strongly reduced and both free and esterified cholesterol levels in the plasma are largely decreased[20,35]. The severe hypocholesterolemia in *APOAI*$^{-/-}$ mice is associated with normal free cholesterol levels in the peripheral tissues but reduced levels of CE, particularly in steroidogenic tissues (*e.g.* adrenals)[35]. The skin is one of the main reservoirs of HDL in the body[21]. Yet, the reduced levels of circulating HDL particles and associated hypolipidemia did not affect the epidermal cholesterol content or general morphology of the skin of mice lacking APOAI[20]. The expression of key genes involved in skin cholesterol synthesis (*HMGCR, HMGCS1*) and lipoprotein uptake (*LDLR, SR-BI*) was strongly upregulated. This data suggests that local cholesterol content is maintained with a combination of increased: (1) local synthesis and (2) uptake of lipids from apolipoprotein B-containing lipoproteins. Importantly, it also indicates that that HDL is not essential for skin reverse transport of lipids but likely plays a role in the delivery of essential lipids to the skin.



Previous studies assessed the lipid composition of whole skin in *APOAI*$^{-/-}$ mice using enzymatic colorimetric assays but, in line with our findings, no differences were observed between the WT control and the *APOAI*$^{-/-}$ counterparts[20]. To our knowledge, we describe for the first time the detailed analysis of the compositions of CERs and FFAs in the epidermis of *APOAI*$^{-/-}$ mice using a LC/MS method, providing detailed information on subclass and chain length of these lipids. Alterations in the CER subclasses and chain length can lead to a less favorable organization of the SC lipids impacting the barrier function of the skin[31,36]. Similar effects have been described for changes in FFA chain length, in particular towards shorter FFA chains (below 24 carbons atoms)[33]. In line, with our method we demonstrate similar profiles of CER subclasses and FFA chain length distribution in the epidermis of WT and *APOAI*$^{-/-}$ mice. Tissues acquire substantial amounts of FFAs from plasma triglycerides and CEs. *APOAI*$^{-/-}$ mice show not only a reduction in plasma CEs, but also lower plasma triglycerides levels. Accordingly, it is unlikely that in the hypocholesterolemic *APOAI*$^{-/-}$ mice CERs and FFAs are maintained by increased uptake of triglycerides from the circulation. The expression of *FAS* and *ACC* (encoding for key enzymes in the fatty acid synthesis) were increased indicating compensatory epidermal fatty acid synthesis[37]. Moreover, the skin of *APOAI*$^{-/-}$ mice displayed reduced mRNA levels of *DGAT2*, encoding for the enzyme involved in the synthesis of triglycerides, thereby lowering the storage of FFA in the form of triglycerides[38]. Interestingly, Arnaboldi *et. al.* (2015) showed with colorimetric assays that also triglyceride and phospholipid content was preserved in the skin of *APOAI*$^{-/-}$ mice[20]. However, the mechanism underlying the preservation of the triglyceride levels in the skin of these mice remains unclear. Hence, our data indicate adaptations in lipid synthesis and uptake in the skin of *APOAI*$^{-/-}$ mice contributing to maintenance of local barrier lipid homeostasis. The organization of the epidermal lipids can be directly

influenced by changes in the barrier lipid composition. Consequently, the lateral lipid organization in the skin of *APOAI*$^{-/-}$ mice (orthorhombic packing) resembles that of the WT control as anticipated.

Other dyslipidemic double-knockout mouse models have been developed combining the hypolipidemic *APOAI*$^{-/-}$ background with an impaired metabolism of apolipoprotein B-containing lipoproteins (*LDLR*$^{-/-}$ and *APOE*$^{-/-}$ mice)[20,39,40]. Upon ageing or when challenged with a high fat/cholesterol diet, skin of the double-knockout *APOAI*$^{-/-}$/*LDLR*$^{-/-}$ model displays accumulation of both free and esterified cholesterol and marked inflammation[39,40]. In contrast, the double-knockout *APOAI*$^{-/-}$/*APOE*$^{-/-}$ mice develop similar dermatological alterations spontaneously in time when on a low-fat diet[20]. Deficiency of ATP-binding cassette A1 (ABCA1) results in hypolipidemia similar to that described for *APOAI*$^{-/-}$ mice, also without the development of any evident skin phenotypes[41]. However, the double-knockouts *ABCA1*$^{-/-}$/*LDLR*$^{-/-}$ on a lipid rich diet and *ABCAI*$^{-/-}$/*APOE*$^{-/-}$ show alterations in their skin comparable to those reported for the double knockouts in *APOAI*$^{-/-}$ background under similar circumstances[41].

The dermatological phenotypes in the *APOAI*$^{-/-}$/*LDLR*$^{-/-}$ on lipid rich diet and *APOAI*$^{-/-}$/*APOE*$^{-/-}$ mice are likely largely driven by the impaired metabolism of apoB-containing lipoproteins leading to a hypercholesterolemic phenotype. The skin lipid composition of mild hypercholesterolemic *LDLR*$^{-/-}$ mice on low fat/cholesterol diet did not differ from WT controls on that diet[25]. However, the skin of *APOE*$^{-/-}$ mice, with a more severe hypercholesterolemic phenotype under the same dietary conditions, showed an FFA profile enriched in short and unsaturated FFA species; thus, evidencing impact of apoB-containing lipoproteins levels on the skin[25]. It is important, however, to note that the dermatological alterations in skin of double knockout *APOAI*$^{-/-}$/*LDLR*$^{-/-}$ and *APOAI*$^{-/-}$/*APOE*$^{-/-}$ mice were more severe as compared to the single knockout *LDLR*$^{-/-}$ on a high fat/cholesterol diet or *APOE*$^{-/-}$ mice, indicating that absence of HDL might enhance the skin phenotype under hypercholesterolemic conditions. In contrast to mice that transport the majority of cholesterol in HDL, humans display high levels of LDL cholesterol[34]. Therefore, it might deem relevant to study the barrier lipid composition of individuals with APOAI polymorphism to better understand how HDL lipids and its metabolism can affect the skin in humans.

To conclude, we showed that hypoalphalipoproteinemia in *APOAI*$^{-/-}$ mice does not affect the skin morphology and that the epidermal lipid profile under hypolipidemic conditions is likely maintained by local compensatory mechanisms in the skin. Our data also suggest that HDL particles are a source of extracutaneous lipids and that the skin lipid profile warrants further investigation in patients with HDL-related dyslipidemias.

**ACKNOWLEDGEMENTS**

We thank Dr. A. B. Ouweneel for providing us the skin of the *APOAI*$^{-/-}$ mice. This research was funded by Leiden Academic Center for Drug Research (LACDR), Leiden University.

## REFERENCES

1. Kosmas, C. E. et al. High-density lipoprotein (HDL) functionality and its relevance to atherosclerotic cardiovascular disease. Drugs Context 7, 1–9 (2018).

2. Lewis, G. F. & Rader, D. J. New Insights Into the Regulation of HDL Metabolism and Reverse Cholesterol Transport. Circ. Res. 96, 1221–1232 (2005).

3. Zannis, V. I., Chroni, A. & Krieger, M. Role of apoA-I, ABCA1, LCAT, and SR-BI in the biogenesis of HDL. J. Mol. Med. 84, 276–294 (2006).

4. Jonas, A. Lecithin cholesterol acyltransferase. Biochim. Biophys. Acta - Mol. Cell Biol. Lipids 1529, 245–256 (2000).

5. Jiang, Y. J., Lu, B., Kim, P., Elias, P. M. & Feingold, K. R. Regulation of ABCA1 expression in human keratinocytes and murine epidermis. J. Lipid Res. 47, 2248–2258 (2006).

6. Jiang, Y. J. et al. Regulation of ABCG1 expression in human keratinocytes and murine epidermis. J. Lipid Res. 51, 3185–3195 (2010).

7. Tsuruoka, H. et al. Scavenger receptor class B type I is expressed in cultured keratinocytes and epidermis. Regulation in response to changes in cholesterol homeostasis and barrier requirements. J. Biol. Chem. 277, 2916–2922 (2002).

8. Ponec, M., Weerheim, A., Lankhorst, P. & Wertz, P. New acylceramide in native and reconstructed epidermis. J. Invest. Dermatol. 120, 581–588 (2003).

9. Haruta-Ono, Y. et al. Orally administered sphingomyelin in bovine milk is incorporated into skin sphingolipids and is involved in the water-holding capacity of hairless mice. J. Dermatol. Sci. 68, 56–62 (2012).

10. Abd El-Latif, M. I. A., Murota, H., Terao, M. & Katayama, I. Effects of a 3-hydroxy-3-methylglutaryl coenzyme A reductase inhibitor and low-density lipoprotein on proliferation and migration of keratinocytes. Br. J. Dermatol. 128–137 (2010). doi:10.1111/j.1365-2133.2010.09694.x

11. Khnykin, D., Miner, J. H. & Jahnsen, F. Role of fatty acid transporters in epidermis: Implications for health and disease. Dermatoendocrinol. 3, 53–61 (2011).

12. Lin, M.-H. & Khnykin, D. Fatty acid transporters in skin development, function and disease. Biochim. Biophys. Acta 1841, 362–8 (2014).

13. Martins Cardoso, R. et al. Hyperalphalipoproteinemic scavenger receptor BI knockout mice exhibit a disrupted epidermal lipid barrier. Biochim. Biophys. Acta - Mol. Cell Biol. Lipids 1865, 158592 (2020).

14. Chroni, A., Duka, A., Kan, H.-Y., Liu, T. & Zannis, V. I. Point Mutations in Apolipoprotein A-I Mimic the Phenotype Observed in Patients with Classical Lecithin:Cholesterol Acyltransferase Deficiency †. Biochemistry 44, 14353–14366 (2005).

15. Huang, W. et al. A Novel Homozygous Missense Mutation in the Apo A-I Gene With Apo A-I Deficiency. Arterioscler. Thromb. Vasc. Biol. 18, 389–396 (1998).

16. Miettinen, H. E. et al. Apolipoprotein A-I FIN (Leu159→Arg) Mutation Affects Lecithin. Arterioscler. Thromb. Vasc. Biol. 17, 3021–3032 (1997).

17. Hovingh, G. K. et al. A novel apoA-I mutation (L178P) leads to endothelial dysfunction, increased arterial wall thickness, and premature coronary artery disease. J. Am. Coll. Cardiol. 44, 1429–1435 (2004).

18. Miller, M., Aiello, D., Pritchard, H., Friel, G. & Zeller, K. Apolipoprotein A-I Zavalla (Leu 159 →Pro). Arterioscler. Thromb. Vasc. Biol. 18, 1242–1247 (1998).

19. Tiniakou, I. et al. Natural human apoA-I mutations L141R Pisa and L159R FIN alter HDL structure and functionality and promote atherosclerosis development in mice. Atherosclerosis 243, 77–85 (2015).

20. Arnaboldi, F. et al. High-density lipoprotein deficiency in genetically modified mice deeply affects skin morphology: A structural and ultrastructural study. Exp. Cell Res. 338, 105–112 (2015).

21. Huang, L. et al. Interleukin-17 Drives Interstitial Entrapment of Tissue Lipoproteins in Experimental Psoriasis. Cell Metab. 29, 475-487.e7 (2019).

22. Ouweneel, A. B., van der Sluis, R. J., Nahon, J. E., Van Eck, M. & Hoekstra, M. Simvastatin treatment aggravates the glucocorticoid insufficiency associated with hypocholesterolemia in mice. Atherosclerosis 261, 99–104 (2017).

23. Out, R. et al. Macrophage ABCG1 Deletion Disrupts Lipid Homeostasis in Alveolar Macrophages and Moderately Influences Atherosclerotic Lesion Development in LDL Receptor-Deficient Mice. Arterioscler. Thromb. Vasc. Biol. 26, 2295–2300 (2006).

24. Boiten, W., Absalah, S., Vreeken, R., Bouwstra, J. & van Smeden, J. Quantitative analysis of ceramides using a novel lipidomics approach with three dimensional response modelling. Biochim. Biophys. Acta - Mol. Cell Biol. Lipids 1861, 1652–1661 (2016).

25. Martins Cardoso, R. et al. Hypercholesterolemia in young adult APOE −/− mice alters epidermal lipid composition and impairs barrier function. Biochim. Biophys. Acta - Mol. Cell Biol. Lipids 1864, 976–984 (2019).

26. Motta, S. et al. Ceramide composition of the psoriatic scale. BBA - Mol. Basis Dis. 1182, 147–151 (1993).

27. Chomczynski, P. & Sacchi, N. The single-step method of RNA isolation by acid guanidinium thiocyanate–phenol–chloroform extraction: twenty-something years on. Nat. Protoc. 1, 581–585 (2006).

28. Gordon, C. J. The mouse: An "average" homeotherm. J. Therm. Biol. 37, 286–290 (2012).

29. Gordon, C. J. The mouse thermoregulatory system: Its impact on translating biomedical data to humans. Physiol. Behav. 179, 55–66 (2017).

30. Mei, J. et al. Body temperature measurement in mice during acute illness: implantable temperature transponder versus surface infrared thermometry. Sci. Rep. 8, 3526 (2018).

31. Janssens, M. et al. Increase in short-chain ceramides correlates with an altered lipid organization and decreased barrier function in atopic eczema patients. J. Lipid Res. 53, 2755–2766 (2012).

32. Danso, M. et al. Altered expression of epidermal lipid bio-synthesis enzymes in atopic dermatitis skin is accompanied by changes in stratum corneum lipid composition. J. Dermatol. Sci. 88, 57–66 (2017).

33. van Smeden, J. et al. The importance of free fatty acid chain length for the skin barrier function in atopic eczema patients. Exp. Dermatol. 23, 45–52 (2014).

34. Kaabia, Z. et al. Plasma lipidomic analysis reveals strong similarities between lipid fingerprints in human, hamster and mouse compared to other animal species. Sci. Rep. 8, 15893 (2018).

35. Plump, A. S. et al. ApoA-I knockout mice: Characterization of HDL metabolism in homozygotes and identification of a post-RNA mechanism of apoA-I up-regulation in heterozygotes. J. Lipid Res. 38, 1033–1047 (1997).

36. van Smeden, J. et al. Intercellular Skin Barrier Lipid Composition and Organization in Netherton Syndrome Patients. J. Invest. Dermatol. 134, 1238–1245 (2014).

37. Kim, C.-W. et al. Acetyl CoA Carboxylase Inhibition Reduces Hepatic Steatosis but Elevates Plasma Triglycerides in Mice and Humans: A Bedside to Bench Investigation. Cell Metab. 26, 394-406.e6 (2017).

38. Roe, N. D., Handzlik, M. K., Li, T. & Tian, R. The Role of Diacylglycerol Acyltransferase (DGAT) 1 and 2 in Cardiac Metabolism and Function. Sci. Rep. 8, 4983 (2018).

39. Wilhelm, A. J. et al. Apolipoprotein A-I Modulates Regulatory T Cells in Autoimmune LDLr −/− , ApoA-I −/− Mice. J. Biol. Chem. 285, 36158–36169 (2010).

40. Zabalawi, M. et al. Inflammation and skin cholesterol in LDLr −/− , apoA-I −/− mice: link between cholesterol homeostasis and self-tolerance? J. Lipid Res. 48, 52–65 (2007).

41. Aiello, R. J. et al. Increased atherosclerosis in hyperlipidemic mice with inactivation of ABCA1 in macrophages. Arterioscler. Thromb. Vasc. Biol. 22, 630–637 (2002).

## SUPPLEMENTARY INFORMATION

## 1. MATERIALS

**Table S1. Forward and reverse primer sequences used for q-PCR.**

| Protein (Gene) | Forward primer Reverse primer |
|---|---|
| Ribosomal protein, large, P0 (RPL0) | CTGAGTACACCTTCCCACTTACTGA CGACTCTTCCTTTGCTTCAGCTTT |
| Ribosomal protein L37 (RPS37) | AGAGACGAAACACTACCGGGACTGG CTTGGGTTTCGGCGTTGTTCCCTC |
| Acetyl-Coenzyme A carboxylase alpha (ACC or ACACA) | GGAAGATGGCGTCCGCTCTGTG GTGAGATGTGCTGGGTCATGTGGAC |
| Ceramide synthase 2 (CERS2) | ACGTGTCTATGCCAAAGCCTCAGATC CGCAGTCGGGTTTTCTCCTTAACATTC |
| Ceramide synthase 3 (CERS3) | GGGCCTCCACGTTTACTGGGGT GCCCTTGGTGCTCTCTGCTTCCT |
| Delta(4)-desaturase, sphingolipid 1 (DEGS1) | GAGCACCATGACTTCCCCAACGTTC CAGGAGTTGTAGTGCGGGAGGTCAT |
| Diacylglycerol O-acyltransferase 2 (DGAT2) | TATTGGTTTCGCCCCCTGCATCTTC ATGTCTTTCTGGGTCGGGTGCTC |
| Elongation of very long chain fatty acids 1 (ELOVL1) | GGCAGAACTTGCCCCTGAGAAGAA TTCACAACAGCCTCCATCCTGGC |
| Elongation of very long chain fatty acids 4 (ELOVL4) | TGGAATCAAGTGGGTGGCTGGAGG AGCATGGTCAGGTATCGCTTCCACC |
| Elongation of very long chain fatty acids 6 (ELOVL6) | GGACCTGTCAGCAAATTCTGGGCTTA GGAGTACCAGGAGTACAGGAGCACA |
| Fatty acid synthase (FAS) | GGCGGCACCTATGGCGAGG CTCCAGCAGTGTGCGGTGGTC |
| 3-hydroxy-3-methylglutaryl-CoA reductase (HMGCR) | CGAGCCACGACCTAATGAAGAATG TGCATCACTAAGGAACTTTGCACC |
| 3-hydroxy-3-methylglutaryl-CoA synthase 1 (HMGCS1) | AAAACACAGAAGGACTTACGCCCGG GTTGCAGGGAGTCTTGGCACTTTCT |
| Involucrin (IVL) | CCTCTGCCTTCTCCCTCCTGTGAGT ACACAGTCTTGAGAGGTCCCTGAACCA |
| Keratin 10 (K10) | GCGGCGACCAATCATCTAAAGGACC CCAGTGGCCCGTATGAAGAGACTCT |
| Low density lipoprotein receptor (LDLR) | TGTGTGATGGAGACCGAGATTG CGTCAACACAGTCGACATCC |
| Stearoyl-Coenzyme A desaturase 1 (SCD1) | TACTACAAGCCCGGCCTCC CAGCAGTACCAGGGCACCA |
| Scavenger receptor class B member I (SR-BI) | AAACAGGGAAGATCGAGCCAGTAG CGTAGTGAAGAACCTGGGGCAT |

## 2. RESULTS

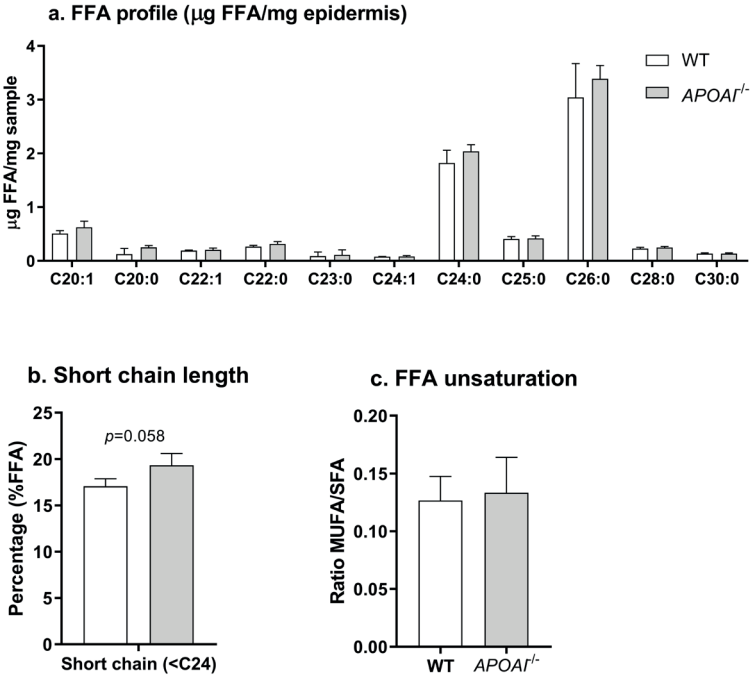


**Figure S1. FFA composition in the skin of WT and *APOAI*$^{-/-}$ mice. A.** Total absolute FFA content in the epidermis depicted according to the carbon chain length. B. The relative abundance of short chain FFAs defined as FFA species with less than 24 carbons. C. Ratio between unsaturated and saturated FFAs. Data shown as mean±SD and plotted (n=3 animals/group).

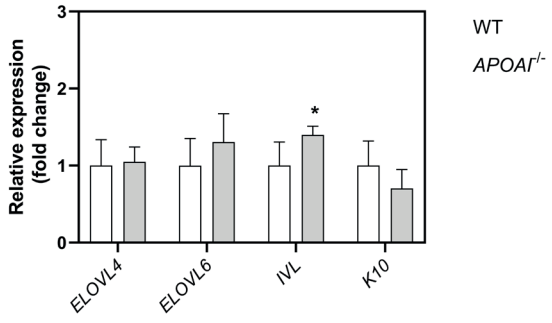


**Figure S2. Gene expression profile in the skin of WT and *APOAI*$^{-/-}$ mice.** Data shown as mean±SD and plotted as fold change expression compared to the WT control (n=5-6 animals/group). Statistical significance was determined by two-tailed unpaired student's t-Test. *$p$<0.05